SLAC – PUB – 3658
April 1985
T

HIGH ENERGY RADIATION FROM NEUTRON STARS*

M. RUDERMAN

Stanford Linear Accelerator Center

Stanford University, Stanford, California, 94305

and

Department of Physics

Columbia University, New York, NY 10027

Invited paper to be published in
Proceedings of the Symposium on Cosmogenic Processes
University of Colorado, March 25-27, 1985
to celebrate the 60th birthday of A.G.W. Cameron

* Research supported in part by the Department of Energy under contract DE-AC03-76SF00515 and a grant from the National Science Foundation

1. Introduction

Neutron stars are observed in two families:

i) isolated, mainly from their non-thermal emission as radiopulsars; these are generally observed as relatively young objects ($\lesssim 10^7$ yrs.);

ii) in binaries, mainly as x-ray sources; these are usually, but not always, old ($\gtrsim 10^7$ yrs). They are usually observed form the thermal x-ray emission associated with accretion from their companions, or from near surface nuclear explosions of the accreted matter.

Isolated radiopulsars from Crablike supernovae explosions have a birthrate of one every few centuries (approximately one for each 5 or so explosions). Their population in our Galaxy $\sim 10^8$. They turn-off as radiopulsars after 10^7 years, so that only about 10^5 are presently observable. Of these almost 400 have now been observed. Neutron stars in binaries appear to have a birthrate of order $10^{-5}\ yr^{-1}$. These are formed in relatively rare events when a supernova explosion does not disrupt the binary. (Some may be formed in relatively mild events when certain White Dwarfs grow beyond their Chandrasekhar limits because of accretion from their companions.) The present Galactic population of neutron stars in binaries $\sim 10^5$. Of order 30-300 of these have been observed as accreting x-ray binaries. If, as in many presently popular models, γ-ray burst sources are also a local population of neutron stars in binaries, at least another 10^2 such neutron star binaries have been detected. The number of observed (and possibly of observable) isolated and binary neutron stars are comparable.

Neutron star surface dipole magnetic fields (B_0) are inferred in a somewhat model dependent way ($B_0^2 \propto P\dot{P}$) from measured radiopulsar stellar spindown

rates ($\dot{P}$) and period (P). The evolutionary track ($\dot{P}$ vs. P) has been measured for only two pulsars, the very young Crab and PSR 1509-58. They give $P\dot{P} \propto P^{\alpha}$ with $\alpha = 0.5$ and 0.2 respectively (Groth 1975, Manchester *et al*, 1985), and are consistent with a $B_0 \sim 3 \cdot 10^{12}$ and $10^{13}\,G$ which grows slightly with time. Most radiopulsars are much older and have a smaller $P\dot{P}$, interpreted as implying $B_0 \sim 10^{12}\,G$; many of these have very much smaller B_0. For the above two very young pulsars $P\dot{P}$ and (perhaps) by implication B_0 will ultimately drop if they are to evolve into typical older pulsars. This is a popular interpretation because there are a number of ways for B_0 to diminish strongly after several million years (an age which is probably comparable to the decay time for crustal currents). We shall consider separately below high energy radiation from young isolated radiopulsars with large B_0 and old ones spun-up in accreting binaries which may, usually, have very small B_0).

2. Young Rapidly Spinning Pulsars

Young pulsars with spindown energy loss rates $\gtrsim 10^{34}\,erg\,s^{-1}$ are embedded in x-ray synchrotron nebulae (Helfand 1982). The nebula radiation is presumably sustained by the injection of energetic e^-/e^+ into the circumstellar magnetic field. For the Vela pulsar this injection rate is $10^{36}s^{-1}$; for the Crab pulsar it is $10^{38}s^{-1}$. These are both several orders of magnitude greater than the maximum ratio of charge separated particle emission from the pulsar itself, limited by the magnetic field of the electric current out of and into the star. This suggests, or is at least consistent with, a currentless flux of $e^{\pm}$ produced near the star as the injected particle source. The assumed production of such an $e^{\pm}$ wind from the near vicinity of the pulsar leads to a successful quantitative description of the

optical and x-ray emission of the Crab nebula (Kennel and Coroniti 1984).

Production of $e^{\pm}$ pairs in the magnetosphere of a young pulsar can be sustained by high energy γ-rays in several ways:

(1) Conversion on strong magnetic fields (Sturrock 1971), important in the very strong magnetic field ($\sim 10^{12}G$) very near the stellar surface;

(2) Conversion to $e^{\pm}$ pairs by collisions with x-rays or other γ-rays;

(3) Conversion by collisions with soft photons (optical or IR), important for $10^{12}eV$ γ-rays.

The energetic γ-rays can be radiated, often by the very e^{+}/e^{-} particles they create, by three mechanisms

(a) Curvature radiation from accelerated e^{-}/e^{+} moving along curved magnetic field lines;

(b) Inverse Compton scattering of extreme relativistic e^{-}/e^{+} on dense soft photon fluxes;

(c) Synchrotron radiation by extreme relativistic electrons moving in tight spirals along $\overrightarrow{B}$.

A test of a young pulsar model is its ability to show how one of the above 3×3 combinations supplies the required $e^{\pm}$ wind from the neutron star.

A second feature of observations of the youngest pulsars is the double pulse structure of the energetic radiation emitted by them. The Crab pulsar gives two cusp shaped subpulses ($\sim 140^{\circ}$ separation) at energies from optical through GeV (Fig. 1) (as well as at radiofrequencies). The spectrum extends to $10^{12}eV$ in at least the "main" pulse (Dowthwaite *et al*, 1984) (Fig. 2). The radiated power $\sim 10^{-3}$ the total spindown energy loss rate of the neutron star. A double pulse

structure ($\sim$ 70° separation) is also present in the observed optical and x-ray pulse structure from LMC 0540-693, a young pulsar in the Large Magellanic Cloud similar in age to the Crab. The Vela pulsar has a double pulsed γ-ray spectrum similar in structure to that from the Crab pulsar ($\sim$ 140° subpulse separation), no, so far observed, x-ray intensity, and only a very weak double pulse optical emission, whose separation ($\sim$ 90°) differs from that of its γ-rays (Fig. 3).

The γ-rays needed to create an $e^{\pm}$ wind and those that are observed directly in double pulses indicate that associated with young high magnetic field rapidly spinning neutron stars are strong and efficient charged particle accelerators. There is no consensus on their structure (or even their location), or on whether they are static accelerators ($\vec{E}$ parallel to $\vec{B}$ and static in a corotating frame) or dynamic (e.g. acceleration by electromagnetic waves).

From observations and models we take the following constraints:

(i) The $e^{\pm}$ production mechanisms and, presumably, the accelerator of the particles which produce the γ-rays needed for them, are effective only at distances from the star $r \lesssim c\Omega^{-1}$ ($\Omega \equiv 2\pi/P$). This follows because all of the above $e^{\pm}$ production mechanisms (a, b, or c) need either large $\vec{B}$ or large fluxes of IR, optical, or x-rays which exist only within such distances of the neutron star.

(ii) The $10^{12} eV$ Crab (and Vela) γ-rays imply an emission distance $r \gtrsim c/3\Omega$; otherwise pair conversion by mechanism (1) in the local $\vec{B}$ will absorb the emitted γ-rays before they can propagate away from the star.

Then *if* $e^{\pm}$ production and γ-ray emission are from the same, or closely contiguous, regions the needed particle accelerator is in the outermagnetosphere ($r \lesssim c\Omega^{-1} \equiv$ light cylinder radius) or the trans-light-cylinder region. (For other

proposed sites for the origin of γ-rays cf. Tademaru 1973, Hardee 1977, Harding *et al.* 1978, Daugherty and Harding 1982).

(iii) The double beams of radiation are rotating fan beams (latitude coverage $\gg$ observed width) rather than cones. If they were cones, the probability for having detected both the Crab and Vela pulsars in searches for pulsars in young supernova remnants would be only about $(1/5) \times (1/5) = 1/25$.

We turn now to models which appear to offer an explanation of these properties and also a quantitative description of the emitted spectra which agrees rather well with the observed ones.

3. "Static Gaps" in Outermagnetospheres

In the laboratory a solid conductor rotating with angular speed $\vec{\Omega}$ has an interior velocity

$$\vec{v} = \vec{\Omega} \times \vec{r} \ , \tag{1}$$

an electric field

$$\vec{E} = \frac{\vec{v}}{c} \times \vec{B} \ , \tag{2}$$

and a charge density

$$\rho = \rho_0 \equiv \frac{\vec{\nabla} \cdot \vec{E}}{4\pi} = \frac{\vec{\Omega} \cdot \vec{B}}{2\pi c} + \text{terms of order } \vec{\nabla} \times \vec{B} \ . \tag{3}$$

From Eq. (2) it follows that

$$\vec{E} \cdot \vec{B} = 0 \tag{4}$$

both in the laboratory and corotating frames. In the corotating frame the interior

potential (V) satisfies

$$\nabla^2 V = 4\pi(\rho - \rho_0) \tag{5}$$

Outside of the spinning solid, $\rho = 0$, $\vec{E} \cdot \vec{B} \neq 0$, and, between distant points near the star, the potential difference $\Delta V \sim \Omega R^2 B c^{-1}$. In the laboratory, maximum rotation speeds for a $10^2 cm$ $10^4 G$ rotator give $\vec{E} \cdot \hat{B}$ outside the rotator ~ 10 Volt cm^{-1}, and $\Delta V \sim 10^3$ Volts, insufficient to pull electrons or ions from the surface. For the Crab pulsar, with $B_0 \sim 3 \cdot 10^{12} G$, the exterior $\vec{E} \cdot \hat{B}$ would be $3 \cdot 10^{12}$ Volt cm^{-1} if the exterior region were to remain empty. This is quite impossible in the presence of such a strong $\vec{E}$ along $\vec{B}$. Charge will be pulled from the star until Eq. (4) is achieved. This in turn would, if achieved, imply Eqs. (1), (2) and (3) for the corotating plasma outside of the star whenever $\rho \neq 0$. Thus the charges in the magnetosphere beyond the star tend to flow until they achieve a rigidly rotating extension of the star. If the magnetosphere were bounded by a thin insulating cylinder which prevented current flow through it (and whose radius is enough less than $c\Omega^{-1}$ that relativistic velocities are not approached) the resulting "static" magnetosphere would satisfy Eqs. (1)-(5). The "static" model charge distribution is indicated in Fig. 4. However, this is not a unique solution. Empty ($\rho = 0$) regions can exist in the magnetosphere, on whose boundaries $\vec{E} \cdot \vec{B} = 0$ so that none of the boundary charge is pulled into them [Holloway 1973, Ruderman and Sutherland 1975, Michel 1981, Cheng *et al.* 1976, Arons 1981]. Some of these are indicated on Fig. 5. There the charge depleted slots are bounded by magnetic field lines along their length. Their ends, however, cross through field lines, but only near the magnetosphere's "null surface" where $\rho_0 = \vec{\Omega} \cdot \vec{B}/2\pi c = 0$ and ρ, in a filled static magnetosphere, changes sign. The exact position and shape of these ends cannot be fixed *a priori* but must be

determined self consistently to give $\vec{E} \cdot \vec{B} = 0$ (Cheng et al 1985a). Within the gap, away from its boundary, $\vec{E} \cdot \vec{B} \neq 0$ and particle acceleration is possible. For a gap which begins and ends within the magnetosphere, the total potential drop (in a corotating frame) from end to end along $\vec{B}$ is zero. Such a gap can be easily filled with charge and is not a source for sustained particle acceleration through it. However a gap along "open" field lines which do not close within the light cylinder may accelerate particles out through the light cylinder and out of the magnetosphere. We now argue that such an "open" gap might be expected to form in a "static" magnetosphere if the insulating cylinder around it were removed so that magnetospheric currents could flow through the light cylinder.

4. "Dynamic Gaps" in Pulsar Outermagnetospheres

If the insulating sheet which, in the "static" magnetosphere approximation, separates the magnetosphere from the rest of the circumstellar region were removed, current would flow along the "open" magnetic field lines through it. If the initial particle flow were only outward through the light cylinder in the general pattern of Fig. 6, this flow would cause a charge depletion region to grow around the null surface. Positive (negative) charge moving out through the light cylinder leaves a void $\rho = 0$ which, according to Eq. (5) has the electrostatic properties of negative (positive) charge in the depleted region. This pushes negative (positive) charge back toward the star from the starward side of the null surface. As the charge depleted regions ("void") grow so does $\vec{E} \cdot \vec{B}$ within them until pair production processes within a "void", of the sort discussed in Section 2, limit further growth by supplying the charge carried away when current flows through the null surface.

Of course when γ-rays from one "void" region propagate through another one the latter void may be quenched by $e^{\pm}$ materialization there. However, all of the processes for making high energy γ-rays give rise only to γ-rays initially directed essentially tangent to the local $\vec{B}$. As a result, a copious γ-ray production from voids in certain regions can quench voids in other regions but not vice-versa. The only void which cannot be quenched because, for geometrical reasons, points within them cannot be reached by high energy γ-rays created near its own (upper) open field line boundary or in other regions are shown in Fig. 6. It is the cross hatched region bounded (below) by the last closed (= first open) magnetic field line, bounded (above) by an open field line boundary, and ending within the magnetiosphere slightly inward of the null surface where the gap $\vec{B} \cdot \vec{B} = 0$. This is an example of the "open" static gap of Section 3 and Fig. 5. There are two such gaps, one on each side of the star.

If, now, the possibility of inward flow through the light cylinder is included, such a gap remains unquenched. It has a roughly constant electric field along $\vec{B}$ through its central region, which falls to zero only at its inner end. Negative (positive) charge sucked into this "outergap" through the light cylinder will be accelerated through the gap and flow down onto the star below. To quench an empty outergap such charges, and oppositely charged ones pulled into the gap from its inner end, would have to stop (or be strongly slowed) within the gap, a behavior quite opposite to their accelerated passage through it. Thus an outergap, as sketched in Fig. 6, once formed, may be stable and continue to grow in thickness until the $\vec{E} \cdot \vec{B}$ through its interior (which, for thin gaps, is proportional to the square of the gap thickness) sustains enough $e^{\pm}$ production near the gap's (upper) open field line boundary to limit further growth. Details

of the structure of such dynamically limited gaps and the energetic radiation from them have been considered by Chen et al. (1985a,b).

5. Pulse Structure of Energetic Radiation Sustained by Outergap Pair Production

Although details of outergap $e^{\pm}$ production can be complicated, and very sensitive to pulsar period, certain feature of the gap related emitted radiation are not. Symmetry of the magnetosphere structure always results in a pair of gaps on opposite sides of the magnetosphere as shown in Fig. 6. The strongest part of that radiation comes from synchrotron and inverse Compton emission by pairs created just above a gap's open field line boundary. a quite general feature of such radiation is that it is mainly emitted in directions almost tangent to the local $\overrightarrow{B}$, and that it is emitted in both tangential directions, reflecting the approximate symmetry between the flow of $e^{-}(e^{+})$ inward and $e^{+}(e^{-})$ outward for all $e^{\pm}$ created within the gap. (This fails, of course, near the gap ends since the total $e^{-}(e^{+})$ current flow there is the sum of all $e^{-}(e^{+})$ creation within the gap and there has not yet been space enough a for large amount of $e^{+}(e^{-})$ production.) The directions of emitted beams are shown in Fig. 7. These are fan beams whose longitudinal extent is, for thin gaps, almost 90°. An observer would see two of them whose arrival time separation comes from difference in time of flight of the radiation across the magnetosphere and from aberration effects since the azimuthal velocity of the local radiating region (Ωr) is typically 0.6 c. The exact pulse time separation depends upon the inclination angle between the stellar spin and magnetic moment and upon the angle between the spin and the observer. Abberation also changes the shape of the emitted beam so that

an observer should see a different (cusped) beam shape from that emitted, at varying r through the beam, in the corotating frame (Fig. 8). The resulting double beam tilted cusp resembles that of the well measured Crab optical profile of Fig. 1. For Vela (but not the Crab) the weak optical radiation originated from closer to the star, where aberration is less, than does the γ-rays. This results in closer optical pulse spacing but the midpoint between pulses (corresponding physically to radiation from $r = 0$) should be the same for all radiation in Vela as observed.

6. Outergap Radiation: Crab Pulsar

A mechanism which is found to limit the growth of the Crab pulsar outergap and to supply enough $e^{\pm}$ pairs to prevent charge depletion elsewhere in the trans-null-surface magnetosphere is the following (Cheng *et al.* 1985b). An e^{+}/e^{-} accelerated through the outergap reaches an energy (limited by radiation reaction) at which it radiates $\sim 10^{5}$ multi-GeV curvature γ-rays per gap passage. These convert to $e^{\pm}$ pairs from collisions with soft x-rays (Section 2, mechanism $2 \cdot a$). When such pairs are created within the gap the e^{+}/e^{-} are separated, accelerated, and repeat the process. Beyond the gap they are unaccelerated and lose their energy by synchrotron radiation (MeV to optical) which supplies the needed x-ray flux through the gap. Inverse Compton scattering of the outside gap $e^{\pm}$ on these same x-ray photons boosts some of them into the MeV-GeV regime. The Crab outergap is limited by this combination of processes when the particle flow through it $\sim 10^{33}\,\mathrm{sec}^{-1}$ and the (related) total potential drop in it along $\overrightarrow{B}$ $\sim 10^{15}$ Volts. The total double fan beam power radiated from the gap transboundary region, which is the source of most of the gap sustained

observed radiation, $\sim 10^{36}\ erg\, s^{-1}$. The total number of created $e^{\pm}$ pairs $\sim$ the total number of multi-GeV curvature γ-rays coming out of the gap (almost all completely converted to $e^{\pm}$ pairs) $\sim 10^5 \times 10^{33}\,\mathrm{sec}^{-1} = 10^{38}\,\mathrm{sec}^{-1}$. This radiated power and $e^{\pm}$ flux are consistent with those which, apparently, come directly from the Crab pulsar. A computed emission spectrum (Ho 1984, Chang *et al.*, 1985), arbitrarily adjusted to fit the integrated intensity, is given in Fig. 9. (The above mechanisms will not give $10 - 12\,eV$ γ-rays. These will be generated in this model by a process which begins with inverse Compton scattering of gap e^-/e^+. The resulting $10^{13}\,eV$ γ-rays will convert in the trans-boundary region into $e^{\pm}$ pairs whose synchrotron radiation is typically in the $10^{12}\,eV$ regime. The beam which must cross the magnetosphere to be observed (beam 3 of Fig. 7) may be absorbed by pair production on the stronger $\overrightarrow{B}$ through which it must pass. In this model the extent of inverse Compton scattering on optical photons deep within the Crab outergap depends upon unknown details of the shape of the heavily plasma loaded magnetic field gap boundary lines near the light cylinder. If such inverse Compton scattering were to be sufficiently large the Crab pulsar outergap might be controlled in part or even mainly by the Vela mechanism of Section 7.

7. Outergap Radiation: The Vela Pulsar

The mechanism $(2 \cdot a)$ which limits the model outergap for Crab parameters is not effective in limiting a similar model outergap for Vela. This is mainly because Vela's outergap synchrotron radiation time scale ($\propto B^{-2} \propto P^6$) is of order 10^3 that of the Crab. There is then insufficient time for Vela $e^{\pm}$ to radiate enough synchrotron photons to sustain the $2 \cdot a$ mechanism for Section 6 before

the radiating pairs flow out of the magnetosphere. Vela, instead, limits its gap in the following, different, way.

In Vela's outergap, each accelerated e^-/e^+ makes of order a hundred $10^{13}\,eV$ γ-rays by inverse Compton scattering on IR ($\sim 10^{-1}\,eV$) photons. These γ-rays then make $e^{\pm}$ pairs on this same IR flux. Some of these pairs are formed in the gap and thus supply e^-/e^+ there to repeat the process. Most convert beyond the gap boundary to give pairs (secondaries) whose crossed beams of synchrotron (secondary) radiation are the observed Vela beams. Additional (tertiary) pairs ($\sim 10^{36}\,\mathrm{sec}^{-1}$) are made by pair-production from the passage of low energy γ-rays of one secondary beam through the highest energy x-rays of the other and vice-versa. These tertiary pairs give the IR synchrotron radiation which flows through the gap and supplies the IR photons whose inverse Compton scattering by gap e^-/e^+ initiates the coupled sequence of outergap controlling processes. Calculations (Cheng *et al* 1985b) give a self limited outer gap for Vela parameters when the secondaries' radiated crossed fan beam power is of order $10^{35}-10^{36}\ erg\,s^{-1}$, and the total (tertiary) pair production rate $\sim 10^{36}\,\mathrm{sec}^{-1}$. The computed emission spectrum, adjusted to fit the total integrated intensity is given in Fig. 10 and compared there to observations. The spectral break at around $10^2\,keV$ occurs because $e^{\pm}$ pairs leave the magnetosphere before their characteristic synchrotron radiation energy falls much below this value. This model spectrum falls below the very weak observed optical intensity if the low energy (optical and IR) radiation from the tertiaries is not included. The latter gives double fan beams (total power $\sim 10^{30}\ erg\,s^{-1}$) emitted from regions enough closer to the neutron star that the pulse interpulse separation is only about 90° (cf. Section 5). In the Vela outergap model the secondaries lose almost all of their energy to synchrotron radiation,

but inverse Compton scattering on the tertiary IR flux does take about 10^{-2} of it. This appears as $10^{12} - 10^{13}\, eV$ γ-rays with total emitted power about 10^{-2} that in the $10^2 - 10^3\, MeV$ band.

This Vela outergap model calculation also suggests that the gap ultimately fills the entire outermagnetosphere region whose $\overrightarrow{B}$ field lines are threaded by the null surface when the spin down energy loss rate of a young pulsar drops to about $10^{34}\ erg\, s^{-1}$. At longer pulsar periods the outergap would no longer be effective in controlling gap size by copious outermagnetosphere $e^{\pm}$ production (cf. Section 1).

8. Radioemission

For Vela radioemission (RF) is presumed to take place much nearer the star, possibly from polar caps at the stellar surface, through mechanisms entirely unrelated to those which support outergap emission. If the surface field is irregular, so are the surface distribution, shape and magnetic field directions of polar caps. Then the observed radiopulse arrival time is unrelated to those of the higher energy outergap emitted pulse and interpulse. But if a somewhat irregular outergap secondary $e^{\pm}$ flow is illuminated by an RF beam which originated elsewhere the beam can be coherently inverse Compton boosted by the motion along $\overrightarrow{B}$ of the moving "mirror" formed by the dense plasma of secondaries, even though the relatively strong local magnetic field strongly suppresses the incoherent scattering of RF by single e^-/e^+. The resulting RF would have a higher frequency than that of the incident beam and be beamed in two directions coincident with those of the higher energy incoherent secondary synchrotron beams from the same $e^{\pm}$ as those which coherently upscattered the incident RF. This suggests the possibility

that the Crab outergap does not create the observed double pulsed RF emission of the Crab pulsar, but merely diverts a precursor like RF beam partially incident upon it.

9. $10^{15}\,eV$ Nucleon Beams from the Crab and Vela Pulsars?

If the relative directions of stellar magnetic moment and spin are such as to give the charge distribution of Fig. 4, a flow of gap accelerated e^- down onto the neutron star surface would pull protons (or positive ions) out of the stellar surface to balance the negative charge of the e^- column. When these protons reach the outergap they will be accelerated through it with negligible energy loss from inverse Compton scattering or curvature radiation. They will, therefore, achieve the full $10^{15}\,eV$ gap potential drop. If emitted from the Vela pulsar such a beam would give no easily observable effect. If emitted from the Crab pulsar, such a beam might be a strong source of $10^{15}\,eV$ γ-rays since 300 eV soft x-rays in the x-ray flux through which the proton passes are at the 300 MeV (center of mass) peak for the $\gamma + p \rightarrow \pi^0 + p$ neutral photoneson production cross section. The calculated superhigh energy γ-ray emission rate from the $\pi^0 \rightarrow 2\gamma$ decay ($\sim 10^{33}\,\mathrm{sec}^{-1}$) would give a flux at the earth of $3 \times 10^{-12}\,cm^{-2}\,s^{-1}$, near that which has been reported from the direction of the Crab (Boone *et al* 1983, Wdowczyk 1984). However $10^{15}\,eV$ γ-rays would not escape from within the Crab light cylinder so the π^0 production cannot be that close to the star.

10. High Energy Radiation during the Accretion Spin-up of Older Neutron Stars

Older isolated neutron stars with smaller $\overrightarrow{B}$ and $\overrightarrow{\Omega}$ would no longer be expected to have Vela (or Crab) type outergaps. However older accreting neutron stars in binaries may, especially during their spin-up phase when the inner part of the accretion disk which feeds them is spinning much more rapidly than the neutron star magnetosphere. If the Crab/Vela "open" outergap exists it is because corotation breaks down: matter outside the light cylinder cannot corotate with the magnetosphere within it and the potential drop between open field lines causes current to flow. If, instead, the outside environment were to rotate faster than the stellar magnetosphere the potential differences and current flow directions would reverse. This is, of course, what happens between the inner accretion disk and the star when there is a large mismatch in angular speed between them. The maximum potential drop which can be developed across the stellar magnetosphere of a slowly rotating neutron star whose magnetic field is penetrated by a surrounding accretion disk is largest when the stellar field is weak enough to permit the inner edge of the accretion disk to just reach the stellar surface, about 10^8 Gauss for an Eddington limit accretion rate ($\dot{m}$) of $10^{18} g s^{-1}$ (Brecher and Chanmugam 1985). In general the maximum magnetosphere potential drop achievable in this way $\sim B_0 (BMR)^{1/2} c^{-1} \sim 10^{16}$ volts. For smaller $\dot{m}$ and/or larger B_0

$$\Delta V \sim (10^{-8} B_0)^{-10/7} (\dot{m}_{18})^{5/7} 10^{16} \text{ Volts} . \qquad (6)$$

This ΔV is comparable to that achieved across the Crab or Vela radiopulsar outergaps only if $B_0 < 10^9 G$ (assuming sub-Eddington accretion, $\dot{m}_{18} < 1$).

Thus potential drops similar to those discussed above for the Crab or Vela may be possible in very low magnetic field accreting neutron stars (presumably of age $\gtrsim 10^7$ years) long before their spins have been spun up to a steady state with their accretion disks.

Because B_0 is small and the accreting stellar surface is hot ($kT \sim keV$), the electrical conductivity across $\vec{B}$ in the star is high enough that stellar ohmic resistivity cannot account for a significant part of ΔV. Despite the large plasma accretion rate the ΔV of Eq. (6) must then be found in the magnetosphere as was true, in part, for the isolated Crab and Vela pulsars. How and where it will give particle acceleration is not yet clear. When $B_0 \sim 10^9 G$, the interface between a slowly rotating neutron star (Ω^*) and the rapidly rotating inner edge of its accretion disk (Ω_a) will probably be the seat of rapid magnetic recombination $[\dot{\vec{B}} \sim (\Omega - \Omega^* \vec{B}]$ and thus of $\Delta V \sim R^2(\Omega_a - \Omega^*) B_0 c^{-1} \sim 10^{16}$ Volts.

Three Galactic objects (in addition to the Crab) have been reported as strong sources of 10^{15} eV γ-rays. If confirmed this would imply accelerators with at least this potential drop. At least two, Vela X-1 (Prothroe *et al.* 1984) and Her X-1 (Baltrusaitis *et al.* 1985) are accreting neutron stars. The third, Cyg X-3, probably is but there are also other theoretical suggestions. Since the nature and period of the condensed object in Cyg V-3 are not yet determined various combinations of stellar P and B_0 can be proposed to give such a ΔV. Her X-1 is a $P = 1.24\,\mathrm{sec}$ x-ray pulsar which is being spun up by an accretion disk fed by Roche lobe overflow by its companion. Vela X-1 has a stellar rotation period $P = 282\,\mathrm{sec}$. Its accretion appears to be fed by the stellar wind of its companion (Henricks 1983) and the large but alternating stellar $\dot{P}$ suggests that the accretion disk formed from the wind close to the neutron star fluctuates in

rotation direction. It is difficult to see how Her X-1 with its 1 sec period and especially how the very slowly rotating Vela X-1 could generate $\Delta V \gtrsim 10^{15}$ Volts unless the accreting disk motion cutting through the stellar B is the potential drop source and B_0 is $\lesssim 10^{10}G$, characteristic of many (and perhaps all) old neutron stars (cf. Brecher and Chanmugam 1985). In such cases "outergap accelerators" may be formed by magnetospheric current flow in old, low B_0, long period neutron stars.

11. Postscript

Seventeen years ago when the initial observations of radiopulsars promoted the theory of neutron stars to a respectable role in astrophysics Al Cameron was among the first to study their internal structure. He introduced several of our colleagues at this conference into a lasting affair with this subject. He has long since moved on to other problems, but uncharacteristically, he forgot to tell those who remain involved with neutron stars what the answers are. Clearly we miss him and wish he were with us.

It is a pleasure to thank Professor S. Drell and the Theoretical Group at SLAC for their very kind hospitality.

FIGURE CAPTIONS

1. Average optical, x-ray and γ-ray pulse profiles of the Crab pulsar (after Manchester and Taylor 1977).

2. γ-ray pulse profile of the Crab pulsar at $10^{12}\,eV$ (Dowthwaite *et al.* 1984) and $10^{8}\,eV$ (Wills *et al.* 1982).

3. Average γ-ray, optical and radio profiles of the Vela pulsar (after Manchester and Taylor 1977 and Kanbach *et al.* 1980).

4. Charge distribution in a "static" magnetosphere of a spinning magnetized neutron star with $\vec{\Omega} \cdot \vec{B} < 0$ above the polar cap. An insulating cylindrical sheet surrounds the magnetosphere and prevents the flow of current through it. (Its surface charge is not shown.) The charge distribution is $\rho \sim \rho_0$ with the negatively charged open field line region shown dotted; $\rho_0 = 0$ on the "null surface" $\vec{\Omega} \cdot \vec{B} = 0$. The closed field lines which do not penetrate the light cylinder ($|\vec{r} \times \vec{\Omega}| = c$) are in the shaded area. $\vec{B}$ field lines are represented by those of a static dipole, a bad approximation near the light cylinder and possibly near the star.

5. Four examples of thin magnetosphere gaps along $\vec{B}$ field lines in a rotating magnetosphere with axial symmetry. All charge has initially been removed from the interior of the gaps (shown cross hatched). In the corotating reference frame these gaps are imbedded in an equipotential conducting plasma. In gap 1 $\vec{E} \cdot \hat{B} < 0$ at the gap ends; negative charge is pulled into the gap through its ends, quickly replenishing the negative charge initially removed and thus destroying the gap. (No charge flows across $\vec{B}$.) In gap 3, $\vec{E} \cdot \hat{B} > 0$ at the gap ends (positive charge was initially removed

there to form that part of the gap) and positive charge flows into the gap to replenish what was initially removed from that gap region. Neither of these gaps is "static". Gap 2 has its end near where $\vec{E} \cdot \hat{B} = 0$ and is "static". If $e^{\pm}$ production existed in it, the $\vec{E} \cdot \hat{B}$ in the gap would accelerate e^{+} toward the gap ends but keep e^{-} bound thus replenishing the gap's charge deficit and annihilating the gap. Gaps of type 4 on open $\vec{B}$ field lines, but whose magnetospheric end is similar to that of gap 2, are the outergaps considered in this paper.

6. A schematic indication of assumed current flow patterns on open field lines. Current flow of positive charge away from the star (mainly via non-charge-separated plasma) is assumed balanced by a return current which is mainly through the "null surface". The inward directed arrow indicates current flow direction only: negative electrons will be *out*flowing in the dotted region. Negative charge is assumed to flow out leaving behind a partial void ($\rho \sim 0$) in the outermagnetosphere near the null surface. The coulomb field of $\rho - \rho_0 \sim -\rho_0$ pushes positive charge on the other side of the null surface toward the star. Pair production processes can fill all voids except the two outergaps shown cross hatched.

7. Model outermagnetosphere with indicated radiation beaming of secondary radiation from four emission regions near the outergap boundary.

8. Effect of aberration in changing the order in which emission from neighboring field lines reaches an observer. A stationary phase exists for the beam from point 2 of beam A. The cusp shape from a similar argument applied to the second pulse (Fig. 7), whose beam traverses the magnetosphere, is shown as B.

9. Model pulse spectra and observed spectrum for the Crab pulsar. [For details and references, see Cheng *et al.* 1985b 1984.] The model integrated intensity is adjusted to fit that observed. The three theoretical curves differ in assumed gap magnetic field and primary e^-/e^+ energy. The solid curve is for $B = 2 \cdot 10^5\, G$ and $E = 10^{13}\, eV$; the dotted curve has $B = 10^6\, G$.

10. Model pulsed spectrum and observed spectrum for the Vela pulsar [for details and references see Cheng *et al* 1985b]. The model integrated intensity is adjusted to fit that observed. Tertiary optical emission (which agrees with that observed) is not included in the theoretical curve. The theoretical curve for modulated x-rays around 1 keV does not include an expected contribution between pulses from thermal polar cap emission. Its existence would raise the observationally derived upper limit by diminishing the amount of observed modulation through the pulse. The three curves correspond to different residence times for secondary pairs in the outermagnetosphere, and/or different synchrotron radiation decay times for these pairs. These determine a minimum for the characteristic energy of synchrotron radiation where there is a break in the spectrum at 80 keV (solid curve), 225 keV (dotted curve), and 575 keV (dashed curve). The uncertain structure of the outermagnetosphere does not support a definitive prediction for the break energy.

REFERENCES

1. Arons, J. 1981 IAU Symposium 74: Origin of Cosmic Rays 175
2. Baltrusaitis, R., Cassiday, G., Cooper, R., Elbert, J., Gerhardy, P., Loh, E., Mizumoto, Y., Sokosky, P., and Steck, D. University of Utah preprint 1985
3. Boone, J., Cady, R., Cassiday, G., Elbert, J., Loh, E., Sokosky, P., Steck, D., Waserbaech, S., 1983 Proceedings of the Cosmic Ray Workshop, University of Utah , p. 268-84
4. Brecher, K. and Chanmugam, G. 1985 Nature 313 767
5. Cheng, A., Ruderman, M., and Sutherland, P., 1976 Ap.J 212 808
6. Cheng, K.-S., Ho, C., and Ruderman, M. 1985a preprint
7. Cheng, K.-S., Ho, C., and Ruderman, M. 1985b preprint
8. Daughterty, J. and Harding, A. 1982 Ap.J 252 337
9. Dowthwaite, J., Harrison, A., Kirkman, I., Macrae, H., McComb, T., Oxford, K., Turner, K., and Walmsley, M., 1984 Ap.J 286 L35.
10. Groth, E., 1975 Ap. J Suppl. 29 431
11. Hardee, p. 1977 Ap.J 216 873
12. Harding, A., Tademaru, E., and Esposito, L. 1978 Ap.J 225 226
13. Holloway, N. 1973 Nature 246 6
14. Helfand, D. 1982, *Supernova Remnants and their X-ray Emission*, IAU Symposium 101
15. Henricks, H. 1983 *Accretion-driven Stellar X-ray Sources* W. Lewin and E. van den Heuvel eds. Cambridge University Press

16. Ho, C. 1984 Columbia University Department of Physics Doctoral Thesis

17. Kanbach, G., Bennet, K., Bignami, G., Buccheri, R., Caraveo, P., D'Amico, N., Hermson, W., Lichti, G., Masnou, J., Mayer-Hasselwander, H., Paul, J., Sacco, B., Swanenberg, B., and Wills, R. 1980 Astron. Astrophys. 90 163

18. Kennel, C., and Coroniti, F. 1984 Ap.J 283 710.

19. Manchester, R., Durdin, J., and Newton, L. 1985 Nature 313 374

20. Manchester, R., and Taylor, J., 1977 *Pulsars*, W. H. Freeman and Co., San Francisco

21. Michel, R. C. 1981 *Pulsars*, IAU Symposium 95 ed. by W. Sieber and R. Wielebinski

22. Protheroe, R., Clay, R., and Gerhardy, P. 1984 Ap.J 280 L47

23. Ruderman, M. and Sutherland, P. 1975 Ap.J 196 51

24. Sturrock, P. 1978 Ap.J 164 529

25. Tademaru, E. 1973 Ap.J 183 625

26. Wills, R. *et al* 182 Nature 296 723

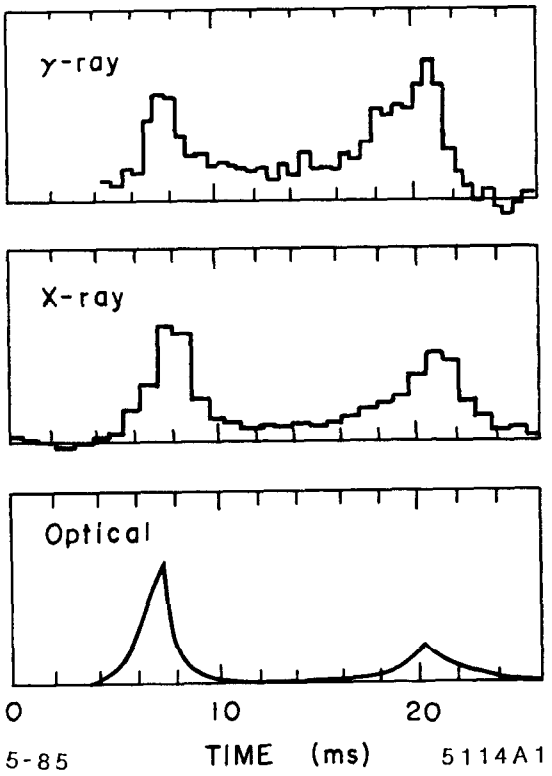

Fig. 1

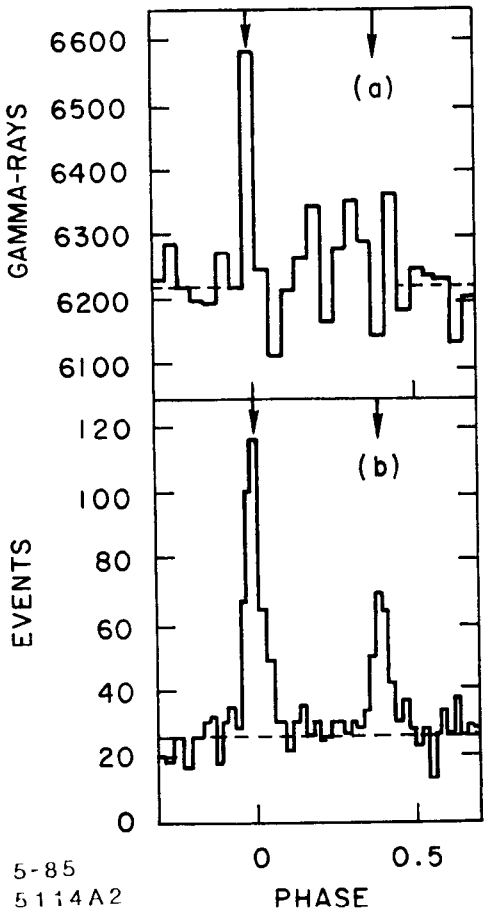
6600
6500
6400
6300
6200
6100
GAMMA-RAYS
(a)
120
100
80
60
40
20
0
EVENTS
(b)
0
0.5
PHASE
5-85
5114A2

Fig. 2

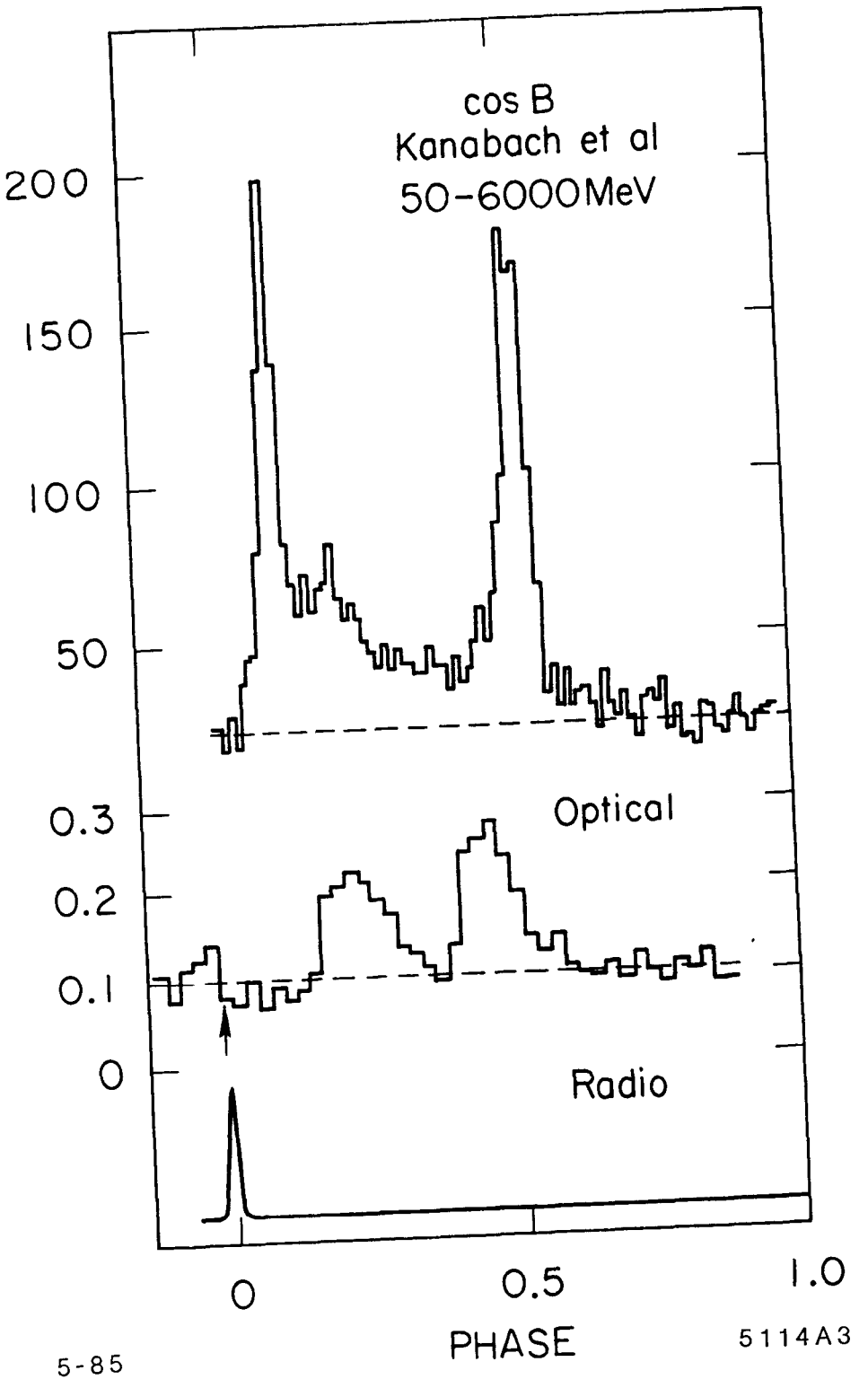
cos B
Kanabach et al
50-6000MeV
200
150
100
50
0.3
0.2
0.1
0
Optical
Radio
0
0.5
1.0
PHASE
5-85
5114A3

Fig. 3

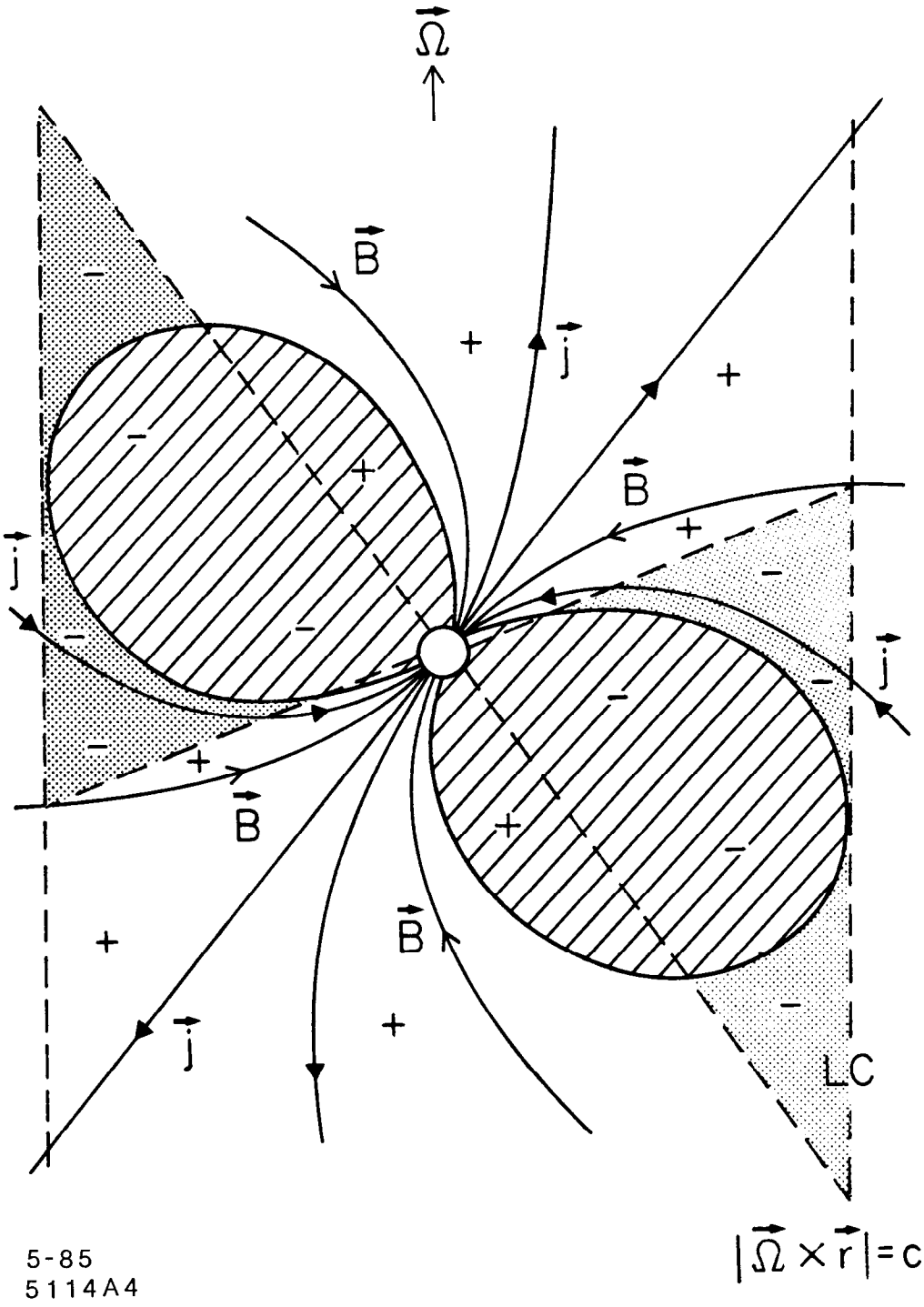

Fig. 4

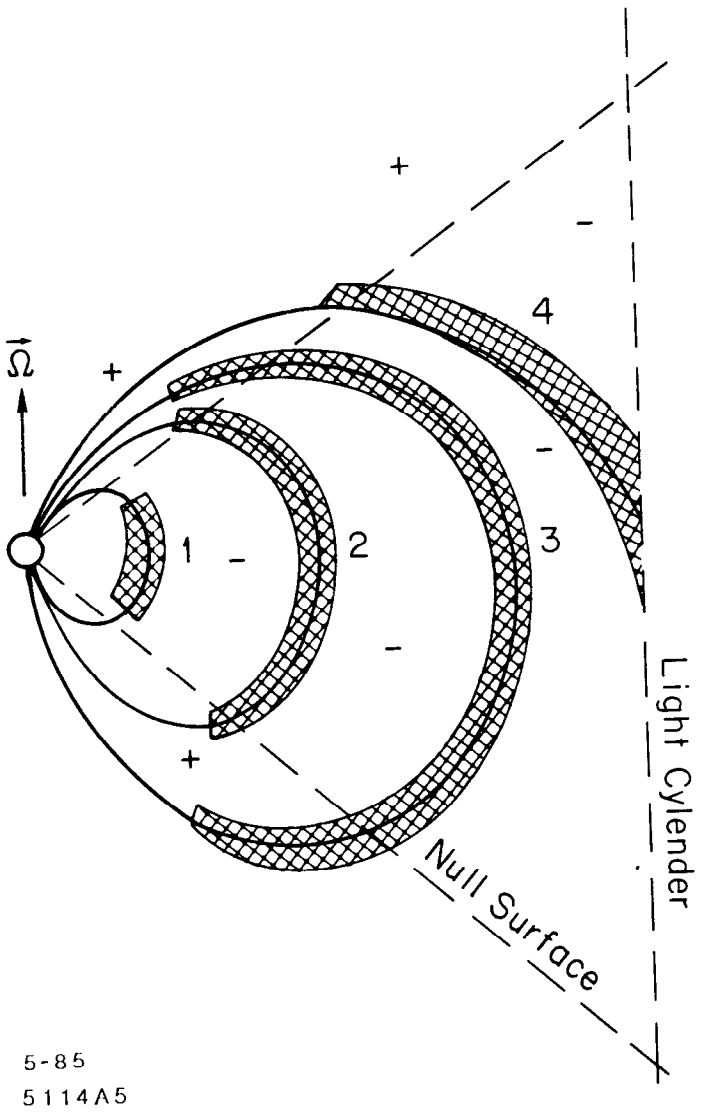

Fig. 5

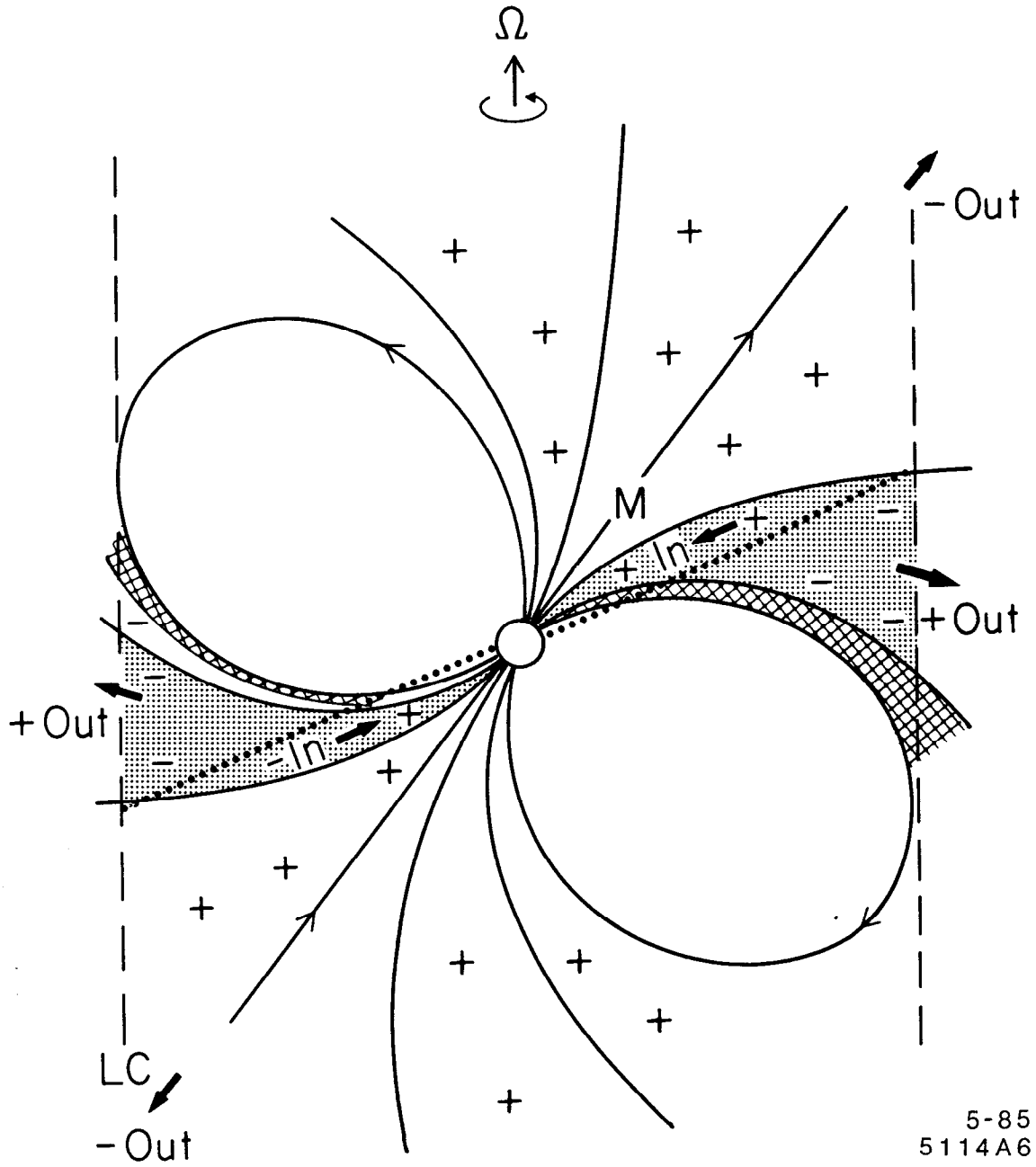

Fig. 6

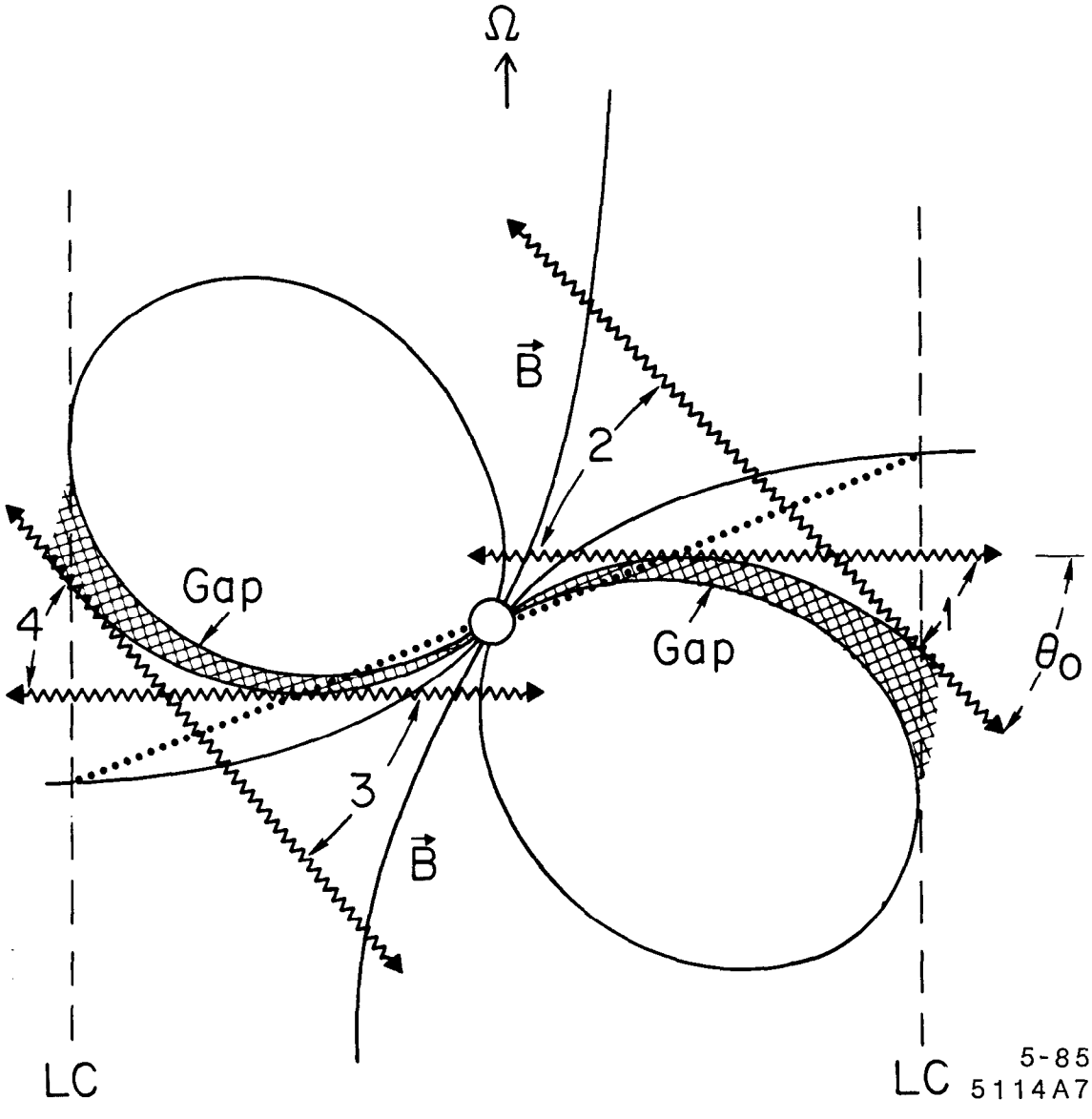

Fig. 7

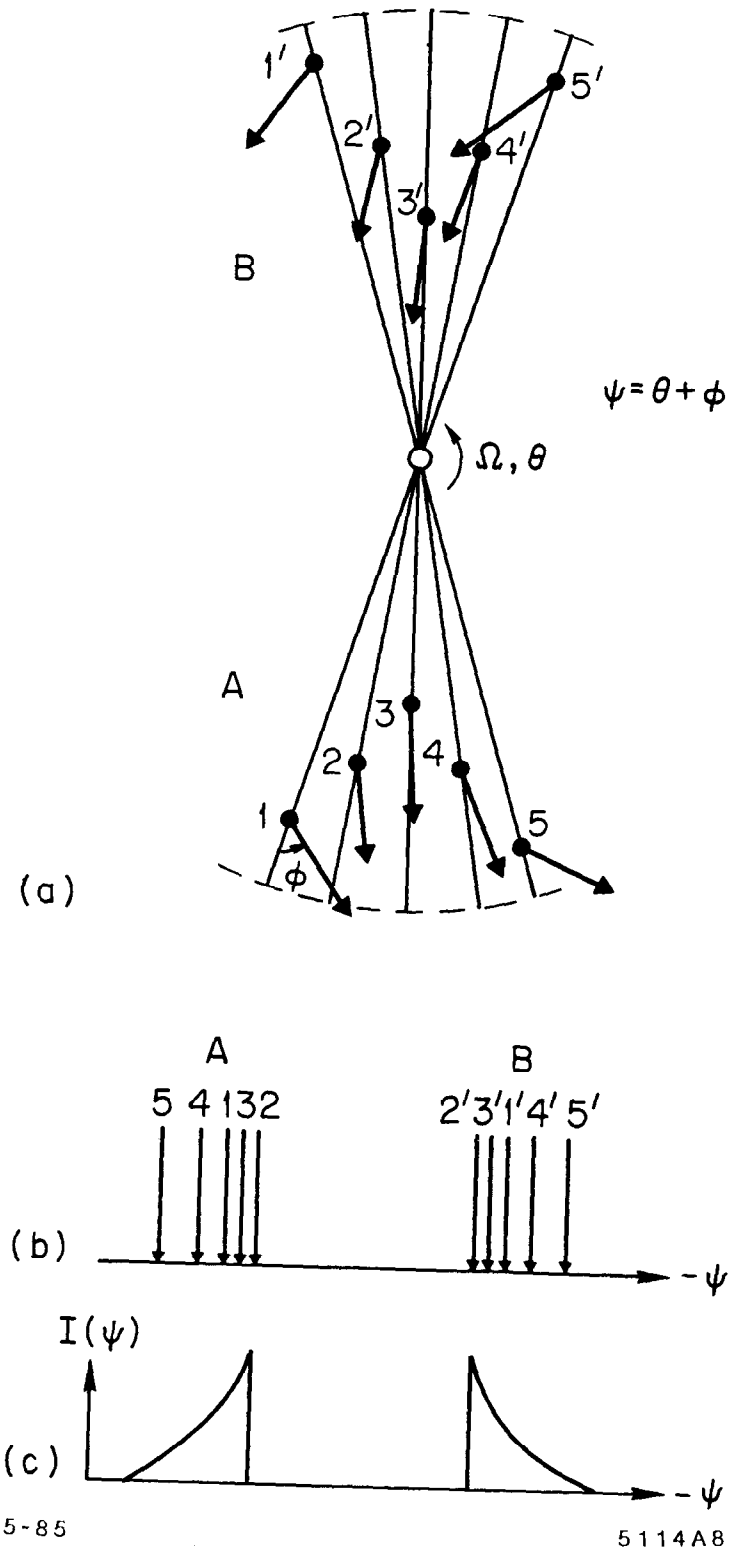

Fig. 8

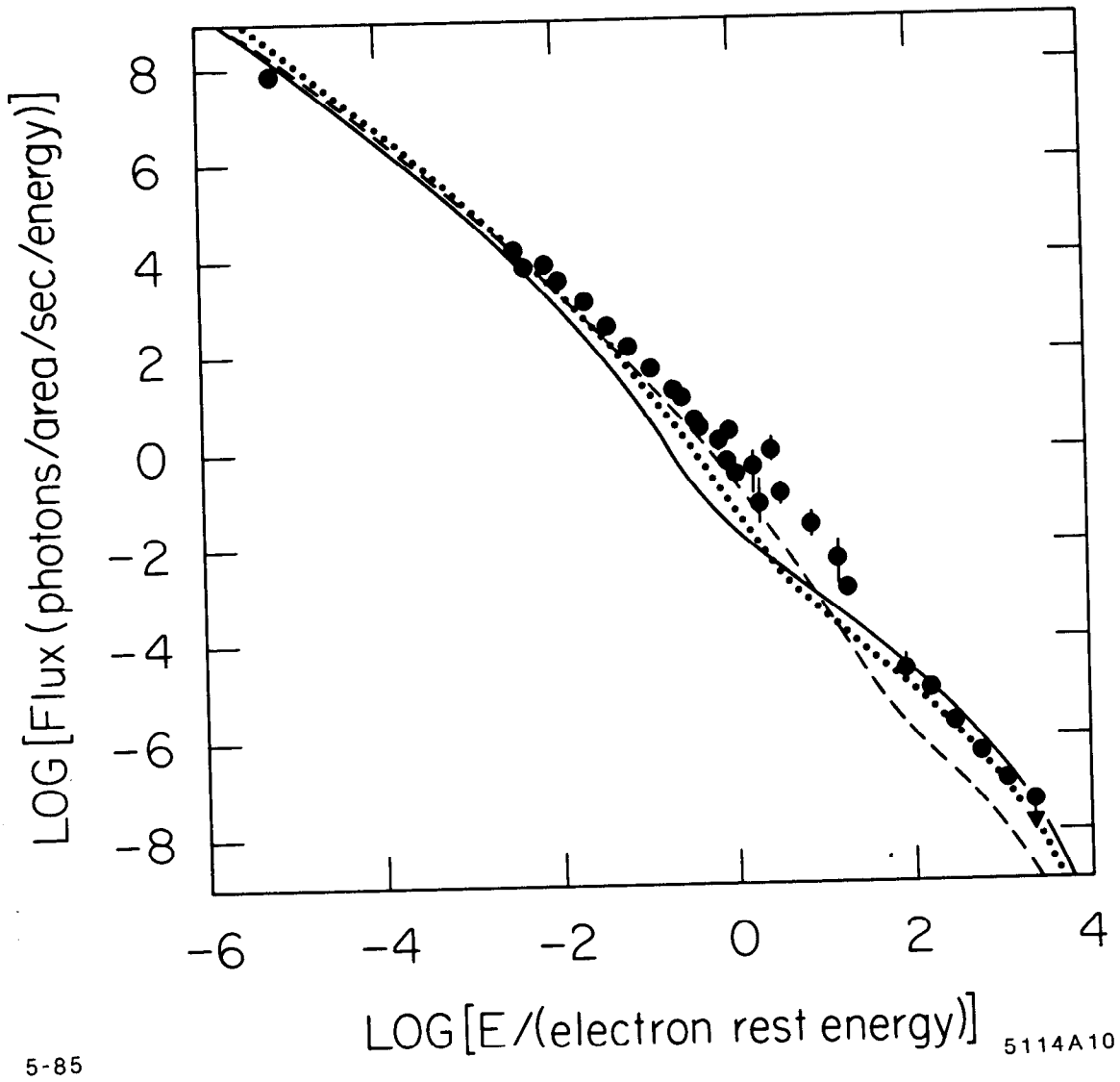
LOG [Flux (photons/area/sec/energy)]
8
6
4
2
0
-2
-4
-6
-8
-6
-4
-2
0
2
4
LOG [E/(electron rest energy)]
5114A10
5-85

Fig. 9

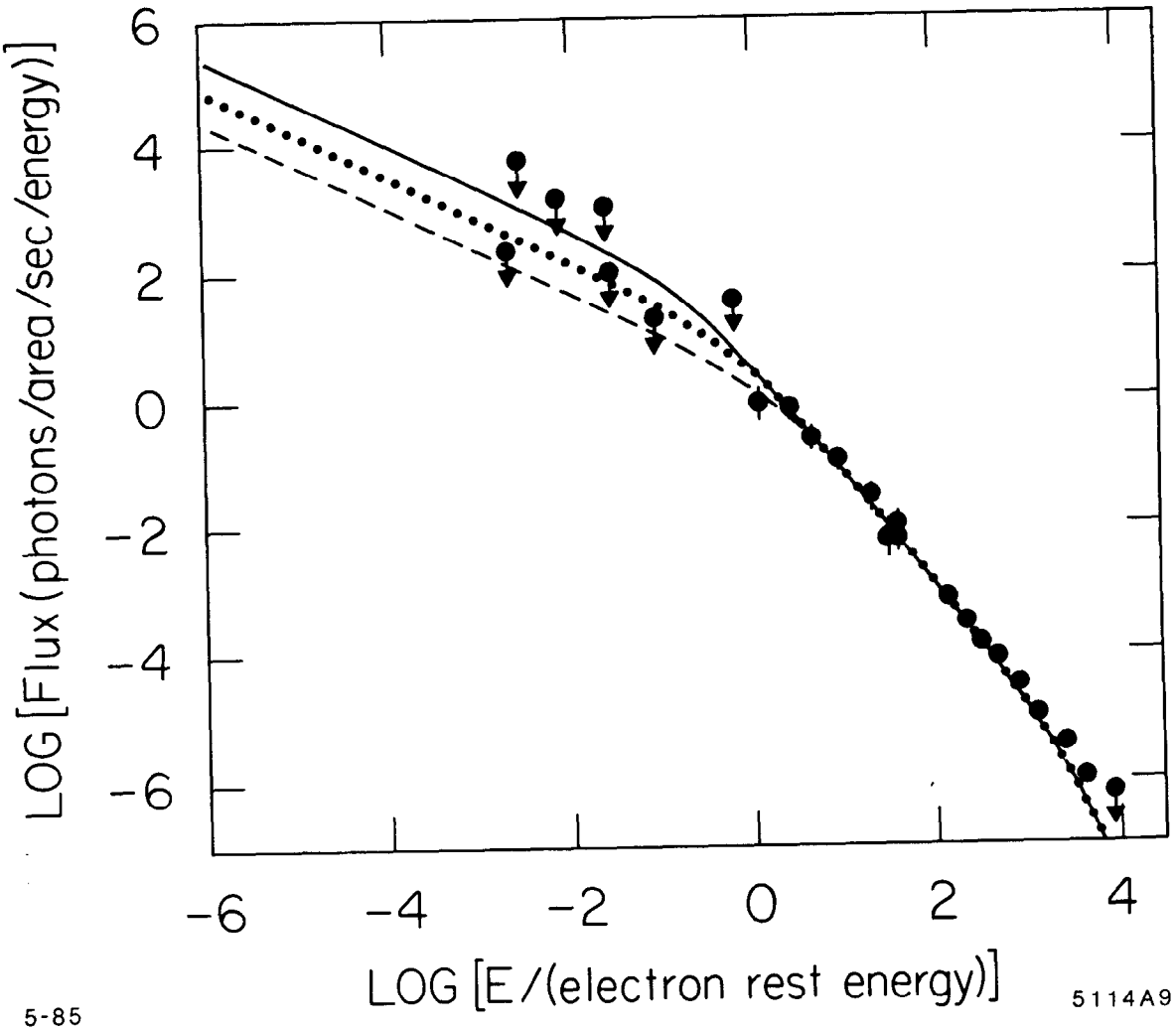
6
4
2
0
-2
-4
-6
LOG [Flux (photons/area/sec/energy)]
-6
-4
-2
0
2
4
LOG [E/(electron rest energy)]
5-85
5114A9

Fig. 10